Hindawi Publishing Corporation
International Journal of Antennas and Propagation
Volume 2015, Article ID 182080, 7 pages
http://dx.doi.org/10.1155/2015/182080

Research Article

Analog Beamforming and Digital Beamforming on Receive for Range Ambiguity Suppression in Spaceborne SAR

Pingping Huang[1] and Wei Xu[2]

[1] *College of Information Engineering, Inner Mongolia University of Technology, Hohhot 010051, China*
[2] *Department of Spaceborne Microwave Remote Sensing, Institute of Electronics, Chinese Academy of Sciences (IECAS), Beijing 100190, China*

Correspondence should be addressed to Pingping Huang; cimhwangpp@163.com

Received 23 October 2014; Accepted 1 February 2015

Academic Editor: Jingjing Zhang

For future spaceborne synthetic aperture radar (SAR) missions, digital beamforming (DBF) on receive in elevation to form a sharp high receive beam will be adopted to improve the signal to noise ratio (SNR) level and suppress range ambiguities. However, in some special cases, range ambiguities may be received by grating lobes with the high receive beam gain, and range ambiguities would not be well suppressed and even may be increased. In this paper, a new receiving approach based on analog beamforming (ABF) and DBF is proposed. According to the spaceborne SAR imaging geometry and the selected pulse repetition frequency (PRF), the antenna patterns of all subapertures of the whole receive antenna in elevation are adjusted by ABF at first. Afterwards, signals from all subapertures in elevation are combined by a real time DBF processor onboard. Since grating lobes could be suppressed by the antenna pattern of the subapertures via ABF, range ambiguities would be well suppressed even if ambiguities are received by grating lobes. Simulation results validate the proposed approach.

1. Introduction

Future spaceborne synthetic aperture radar (SAR) systems require the high resolution wide swath imaging capacity [1–3]. Although the high azimuth geometric resolution and the wide swath pose different pulse repetition pulse frequency (PRF) requirements, this contradiction could be overcome by the azimuth multichannel technique [2–5], which introduces additional spatial samples to reduce the PRF requirement. In addition to overcoming the contradictive PRF requirement, improving the signal to noise ratio (SNR) level and suppressing range ambiguities are very important for spaceborne high resolution wide swath imaging.

To improve the SNR level and suppress range ambiguities, a large size of the planar receive antenna is adopted in elevation. Furthermore, the large receive antenna is divided into multiple subapertures, and echoes of the whole imaged swath are individually received and sampled in individual channel by each subaperture. Afterwards, echoes from all subapertures are combined together by a digital beamforming (DBF) processor [6–9]. Besides adopting the large size of the planar antenna with multiple subapertures, the large size of the reflector antenna is also suggested for the DBF operation in elevation [10–12]. This DBF on receive scheme is to form a narrow sharp receive beam which follows the radar pulse as it travels on the ground. Taking account of the hardware complexity of the spaceborne SAR system, the large receive antenna is divided into a limited number of subapertures [13, 14]. As a result, grating lobes would occur during the radar pulse chasing. In most cases, we need not take care of these grating lobes, since these lobes would not receive any radar echoes. However, in some special cases depending on the relationship between the operated PRF and the side looking SAR imaging geometry, parts of range ambiguities are received by grating lobes with the high antenna gain, which may result in the seriously increased range ambiguity to signal ratio (RASR).

A simple way to suppress the power of grating lobs is that the large receive antenna is divided into more subapertures at cost of the increased system complexity. In this paper, a new receive approach combined with analog beamforming (ABF) in each subaperture and DBF in the whole receive

antenna is proposed. The antenna pattern of each subaperture in elevation is adjusted via ABF to suppress gain of grating lobes, when the range ambiguities are received by grating lobes. Simulation results validate the effect on suppressing the RASR of the proposed approach.

This paper is arranged as follows. Section 2 reviews the DBF on receive approach and analyzes the case of part of range ambiguities received by grating lobes. The proposed receive approach in elevation is presented in Section 3. Afterwards, a simulation experiment of a designed system example is carried out in Section 4. Finally, this paper is concluded in Section 5.

2. DBF on Receive

Similar to the displaced phase center multiple azimuth beams (DPCMAB) technique in azimuth, the large receive antenna in elevation adopted in DBF on receive is also divided into multiple subapertures to receive echoes of the whole illuminated area, and echoes received by each subaperture are individually downconversed and sampled. To avoid a large amount of the raw data to be downlinked, echoes from all subapertures in elevation are combined together by a DBF processor onboard. Actually, this processing scheme implements a range time variant scanning beam which follows the transmitted radar pulse as it travels on the ground, and it is named SCan-On-REceive (SCORE) [6].

To reduce the system complexity and the processing difficulty onboard, the number of subapertures to be divided in elevation is usually very limited. As a result, according to the working principle of the phased array antenna, multiple grating lobes would appear and may become very high during the sharp receiving beam scanning especially for the edge of the swath with a large scanned angle. Figure 1 shows the antenna pattern of the large array antenna, the carrier frequency is 9.6 GHz, the length of the antenna is 1.6 m, the number of subapertures is 8, and the squinted beam pointing direction is 3°.

According to the working principle of the phased array antenna, the angular interval between the main beam pointing direction and the grating lobe pointing direction can be expressed as [15]

$$\Delta\theta_{gl,k} = k \cdot \frac{\lambda}{d_r}, \quad k = \pm 1, \pm 2, \ldots, \tag{1}$$

where k is the serial number of grating lobes, λ is the wavelength, and d_r is the length of the subaperture. Since the antenna pattern of the whole phased array is weighted by the antenna pattern of the subaperture as shown in Figure 1, the first pair of grating lobes are with the highest power and the first pair should be only considered during the system design.

Assuming that a point target P on the ground is with the slant range r_0, the looking angle of the point target P is computed as

$$\theta_0 = \arccos \sqrt{\frac{(R_e + H)^2 + r_0^2 - R_e^2}{2(R_e + H) \cdot r_0}}, \tag{2}$$

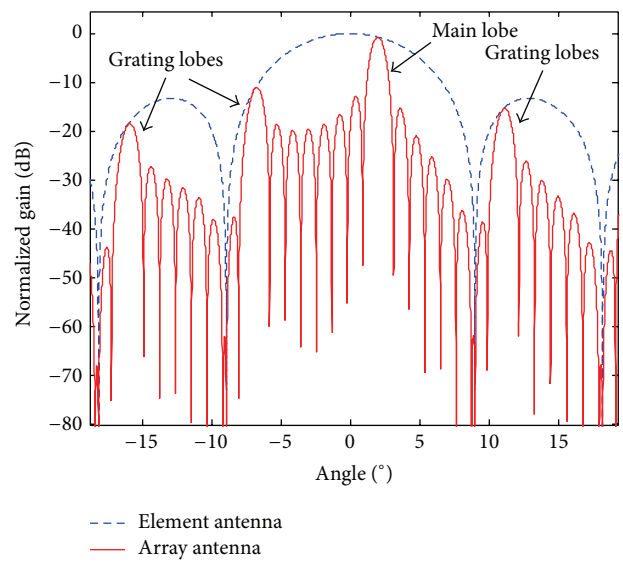

Figure 1: Array antenna pattern with a limited number of subapertures.

where H is the height of the platform and R_e is the radius of the Earth. According to the spaceborne SAR imaging geometry, the mth range ambiguity of the point target P is described by the slant range r_m and the looking angle θ_m as follows:

$$r_m = r_0 + \frac{m \cdot c}{2\mathrm{PRF}}, \quad m = \pm 1, \pm 2, \ldots$$
$$\theta_m = \arccos \sqrt{\frac{(R_e + H)^2 + r_m^2 - R_e^2}{2(R_e + H) \cdot r_m}}, \tag{3}$$

where PRF is the pulse repetition frequency and c is the speed of the light. If the angular interval $\Delta\theta_m = \theta_m - \theta_0$ between the target and its corresponding range ambiguity arriving directions to the receive antenna equals to $\Delta\theta_{gl,1}$, then the corresponding range ambiguity is received by the grating lobe as shown in Figure 2.

3. ABF and DBF on Receive

One of simple ways to resolve the problem of the high range ambiguity due to ambiguities received by grating lobes is changing the operated PRF of the swath. However, this changing sometimes may conflict with the timing diagram selection. Another way is suppressing grating lobes during DBF processing, which results in the main gain reduction and the increased power of sidelobes. Actually, grating lobes could be well suppressed by adjusting the antenna pattern of each subaperture, since the receive antenna pattern $G_r(\theta)$ is written as follows:

$$G_r(\theta) = G_{\mathrm{sub}}(\theta) \cdot \mathrm{A}_{\mathrm{DBF}}(\theta \mid \theta_0), \tag{4}$$

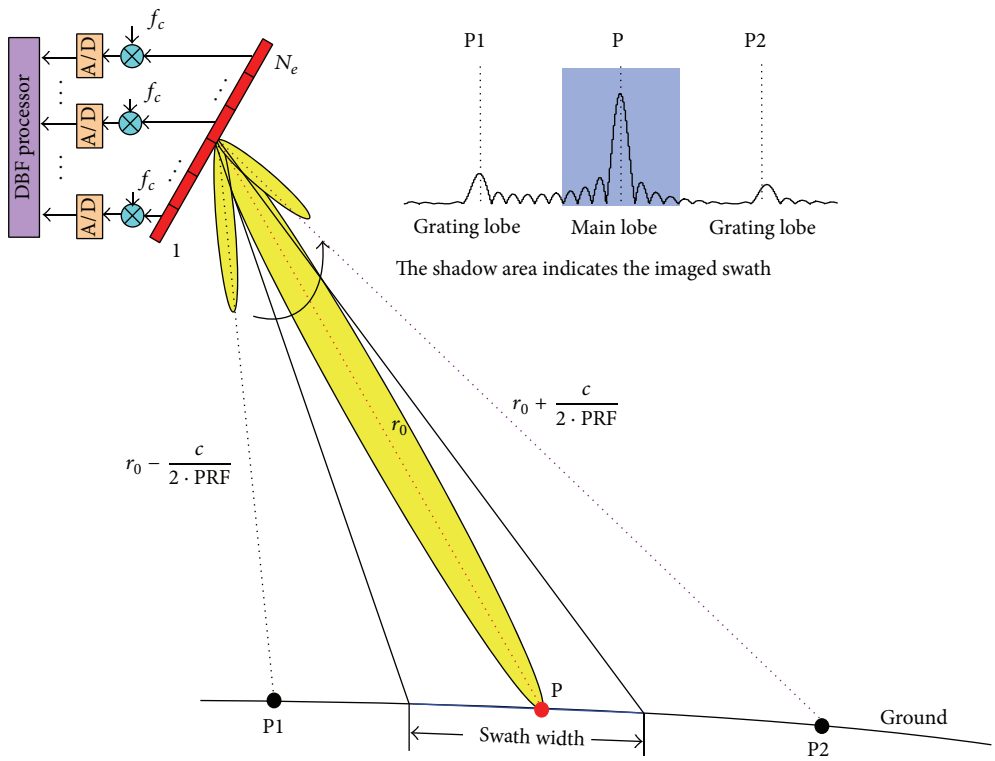

Figure 2: Graphic explanation of range ambiguities received by grating lobes during pulse chasing.

with

$$\mathrm{A}_{\mathrm{DBF}}(\theta \mid \theta_0) = \left| \sum_{n=1}^{N_e} \exp\left\{ j\frac{2\pi}{\lambda}(n-1)\, d_r \left[\sin(\theta) - \sin(\theta_0(t))\right] \right\} \right|, \tag{5}$$

where N_e is the number of subapertures in elevation, while $\theta_0(\tau)$ indicates the fast time τ variant echo reviving direction. Furthermore, each subaperture consists of multiple element antennas which are controlled by the ABF net. As a result, the receive antenna pattern $G_r(\theta)$ is rewritten as follows:

$$\begin{aligned} G_r(\theta) &= G_e(\theta) \cdot \mathrm{A}_{\mathrm{ABF}}(\theta \mid \theta_c) \cdot \mathrm{A}_{\mathrm{DBF}}(\theta \mid \theta_0) \\ &= G_0 \cdot \mathrm{sinc}\left(\frac{\lambda}{d_e}\sin\theta\right) \cdot \mathrm{A}_{\mathrm{ABF}}(\theta \mid \theta_c) \cdot \mathrm{A}_{\mathrm{DBF}}(\theta \mid \theta_0), \end{aligned} \tag{6}$$

with

$$\mathrm{A}_{\mathrm{ABF}}(\theta \mid \theta_c) = \left| \sum_{q=1}^{Q} \exp\left\{ j\frac{2\pi}{\lambda}(q-1)\, d_e \left[\sin(\theta) - \sin(\theta_c)\right] \right\} \right|, \tag{7}$$

where G_0 represents the antenna gain of the element antenna in elevation, d_e is the length of the element antenna, Q is the number of element antennas in each subaperture, and θ_c indicates the center of the imaged swath. To avoid the high RASR level, an additional angular interval $\Delta\theta_r$ is introduced, and the receive antenna pattern becomes

$$\begin{aligned} G_r(\theta) = G_{r,0} \cdot \mathrm{sinc}\left(\frac{\lambda}{d_e}\sin\theta\right) \cdot \mathrm{A}_{\mathrm{ABF}}(\theta \mid (\theta_c + \Delta\theta_r)) \\ \cdot \mathrm{A}_{\mathrm{DBF}}(\theta \mid \theta_0). \end{aligned} \tag{8}$$

This means that the receive beam of each subaperture in elevation is not pointed to the swath center, which may result in the little degradation of the obtained SNR. However, the additional angular interval $\Delta\theta_r$ is very useful to suppress the range ambiguities, since the high grating lobes could be well suppressed by the antenna pattern of the subaperture.

Figure 3 shows the block diagram of ABF and DBF on receive in elevation, which contains two parts: ABF net of each subaperture and DBF net of the whole receive antenna. The ABF net of each subaperture consists of s series of phase shifters, their corresponding phase is expressed as a vector $\boldsymbol{\varphi}_k$ as follows:

$$\begin{aligned} \boldsymbol{\varphi}_k &= [\varphi_{k,1}, \varphi_{k,2}, \ldots, \varphi_{k,M}] \\ &= \left[0, 2\pi\frac{d_e}{\lambda}\sin(\theta_c + \Delta\theta_r - \theta_{\mathrm{mid}}), \ldots, 2\pi(M-1) \right. \\ &\quad \left. \cdot \frac{d_e}{\lambda}\sin(\theta_c + \Delta\theta_r - \theta_{\mathrm{mid}})\right], \end{aligned} \tag{9}$$

where M is the number of phase shifters of each subaperture and θ_{mid} indicates the normal direction of the whole receive antenna. The vector $\boldsymbol{\varphi}_k$ is used to adjust the antenna pattern

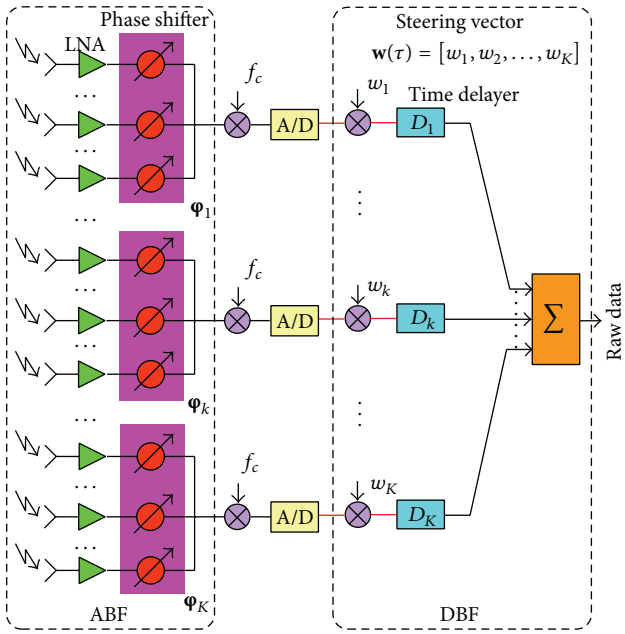

Figure 3: The block diagram of ABF and DBF on receive in elevation.

of the subaperture. For the next DBF step [16], a multiplied complex steering vector $\mathbf{w}(\tau)$ and a time delay vector $\mathbf{D}(\tau)$ representing a series of time delayers are, respectively, given as follows:

$$\mathbf{w}(\tau) = \left[1, \exp\left(j2\pi\frac{d}{\lambda}\sin(\theta_0(\tau) - \theta_{\text{mid}})\right), \ldots, \exp\left(j2\pi(K-1)\frac{d}{\lambda}\sin(\theta_0(\tau) - \theta_{\text{mid}})\right)\right], \tag{10}$$

$$D_k(\tau) = \frac{(k-1)}{c} \cdot d \cdot \sin(\theta(\tau) - \theta_{\text{mid}}) - \frac{(k-1) f_0}{K_r} \tag{11}$$

with

$$f_0 = \frac{d}{\lambda} \cdot \cos(\theta(\tau_c) - \theta_{\text{mid}}) \cdot \frac{\partial\theta(\tau_c)}{\partial\tau}, \tag{12}$$

where K_r is the chirp rate and τ_c indicates the time delay of the swath center.

Figure 4 shows the antenna patterns of the whole receive antenna after ABF and DBF steps. Compared with the antenna pattern without introducing the $\Delta\theta_r$ as shown in Figure 4(a), grating lobes of the whole receive antenna are well suppressed via the adjusted antenna pattern of each subaperture in elevation. Consequently, range ambiguities could be well suppressed even if they would be received by grating lobes according to the side looking SAR imaging geometry.

The aims of DBF in elevation are suppressing range ambiguity and improving the SNR especially for the edge of swath. The range ambiguity to signal ration (RASR) could be computed as follows [17]:

$$\text{RASR}(\eta) = \frac{\sum_{n\neq 0} \sigma(\eta_{\text{amb},n}) \cdot [G_t(\theta_{\text{amb},n}) \cdot G_r(\theta_{\text{amb},n})]^2 / r_n^3 \sin(\eta_{\text{amb},n})}{\sigma(\eta) \cdot [G_t(\theta) \cdot G_r(\theta)]^2 / r_0^3 \sin(\eta)}, \tag{13}$$

with

$$G_t(\theta) = G_{t,0} \cdot \text{sinc}\left[\frac{\pi d_t}{\lambda}\sin(\theta + \Delta\theta_t)\right], \tag{14}$$

where $\sigma(\eta)$ represents the backscattering coefficient, η is the incident angle, and $\theta_{\text{amb},n}$ and $\eta_{\text{amb},n}$ are the looking angel angle and incident angle of the nth ambiguity. The angular offset $\Delta\theta_t$ is usually adopted to improve the SNR level in spaceborne SAR system design. Another important system performance is noise equivalent sigma zero (NESZ), which is computed as follows [17]:

$$\text{NESZ} = \frac{256\pi^3 K T_0 F_n r_0^3 L_{\text{sys}} L_{\text{az}} v_s B_r \sin(\eta)}{P_t G_t(\theta) G_r(\theta) \lambda^3 c \cdot \tau_p \cdot \text{PRF}}, \tag{15}$$

where K is the Boltzmann constant, T_0 is the receiver temperature, F_n is the noise figure, L_{sys} denotes the system losses, L_{az} indicates the azimuth loss, v_s is the satellite velocity, B_r is the transmitted pulse bandwidth, r_0 is the slant range, and τ_p is the pulse duration. To obtain satisfied RASR and NESZ, Figure 5 shows the block diagram of system design for ABF and DBF on receive in elevation. The angular interval $\Delta\theta_t$ for transmitting is introduced to improve the NESZ, while the angular interval $\Delta\theta_r$ in ABF net of each received subaperture is adopted to suppress grating lobes to obtain the desired RASR level.

Table 1: Simulation system parameters.

Parameters	Value
Sensor height	700 km
Carrier frequency	9.65 GHz
Size of the whole antenna (az. × el.)	15 m × 0.72 m
Number of subapertures (az. × el.)	10 × 4
Number of T/R modules (az. × el.)	80 × 36
Pulse duration	80 μs
Pulse bandwidth	500/350/240 MHz
Peak power	64 kw
Looking angle	18°~53°
Swath width	100 km
Overlap between adjacent swaths	⩾5%

4. Simulation Experiment

To validate the effect on the range ambiguity suppression of the proposed receive approach, a designed system example is given in this section. Simulation parameters and performances requirement are listed in Table 1. According to the

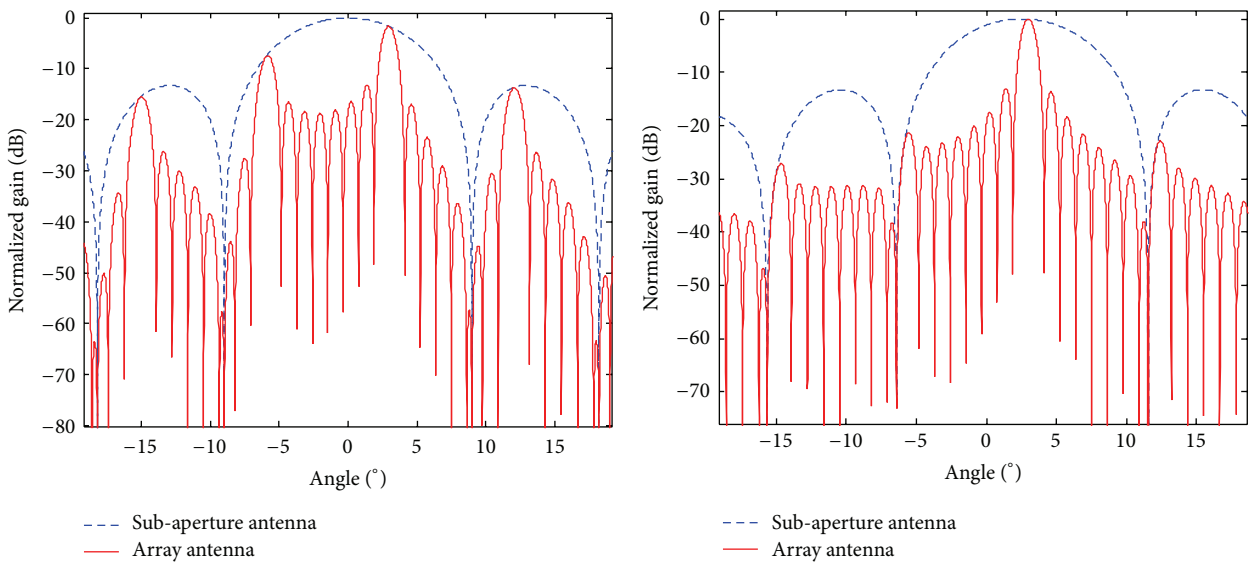

(a) Without subaperture antenna pattern adjusting

(b) Subaperture antenna pattern adjusting

Figure 4: Antenna patterns of the whole receive antenna.

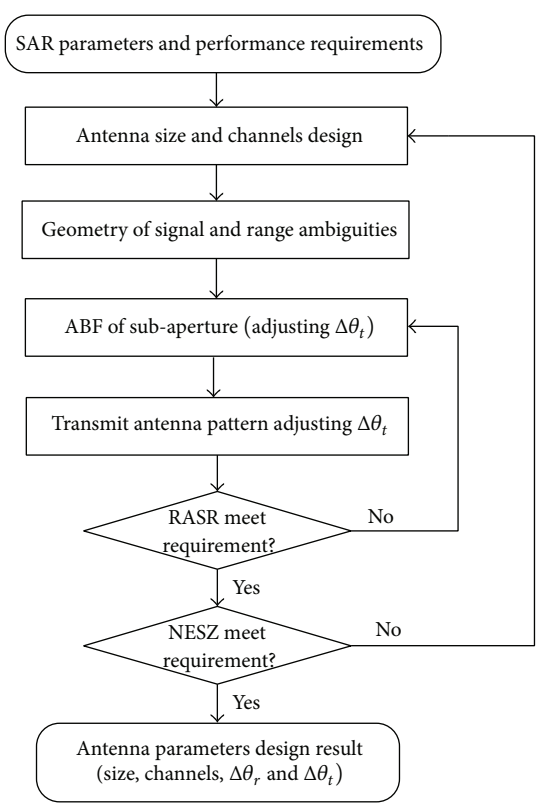

Figure 5: The block diagram of system design for ABF and DBF on receive in elevation.

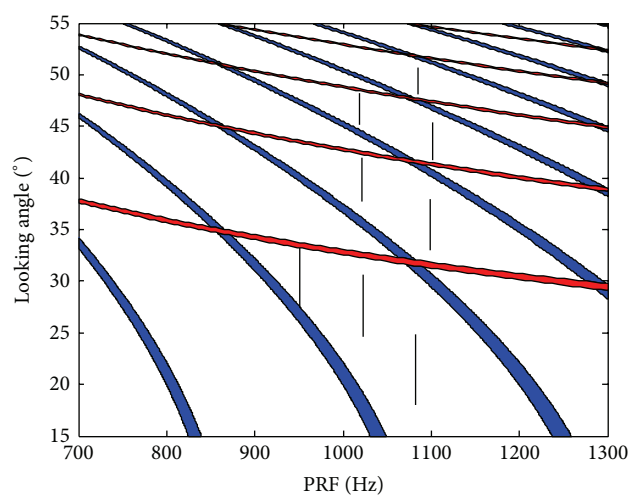

Figure 6: The timing diagram selection result.

simulation system parameters, the timing diagram selection result is shown in Figure 6.

Figure 7 shows system performances RASR and NESZ of all swaths in Figure 6, when conventional DBF on receive in elevation is adopted to improve system performances. Figure 8 shows system performances RASR and NESZ of all swaths with the proposed echo receive approach. It can be seen that the RASR values are obviously improved as shown in Figure 8(a) at the cost of the little NESZ value degradation as shown in Figure 8(b).

5. Conclusion

This paper proposes a receive approach in elevation to reduce the high RASR level in the case of ambiguities received by grating lobes with the high receive gain. Since the antenna pattern of the whole antenna is weighted by the antenna pattern of the subaperture, the antenna pattern

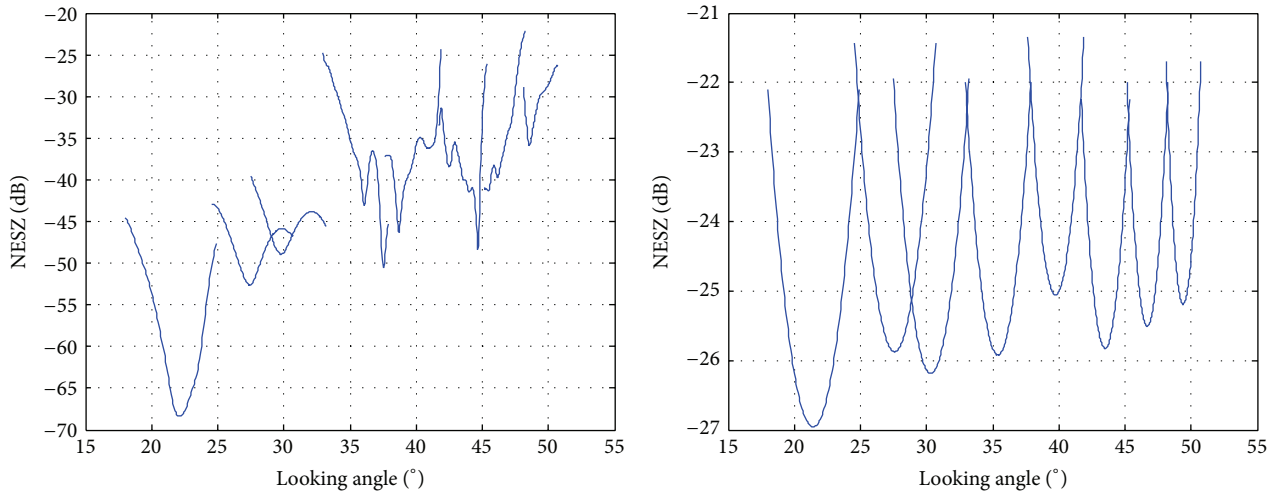

(a) RASR (b) NESZ

Figure 7: System performances of the designed SAR system with conventional DBF on receive.

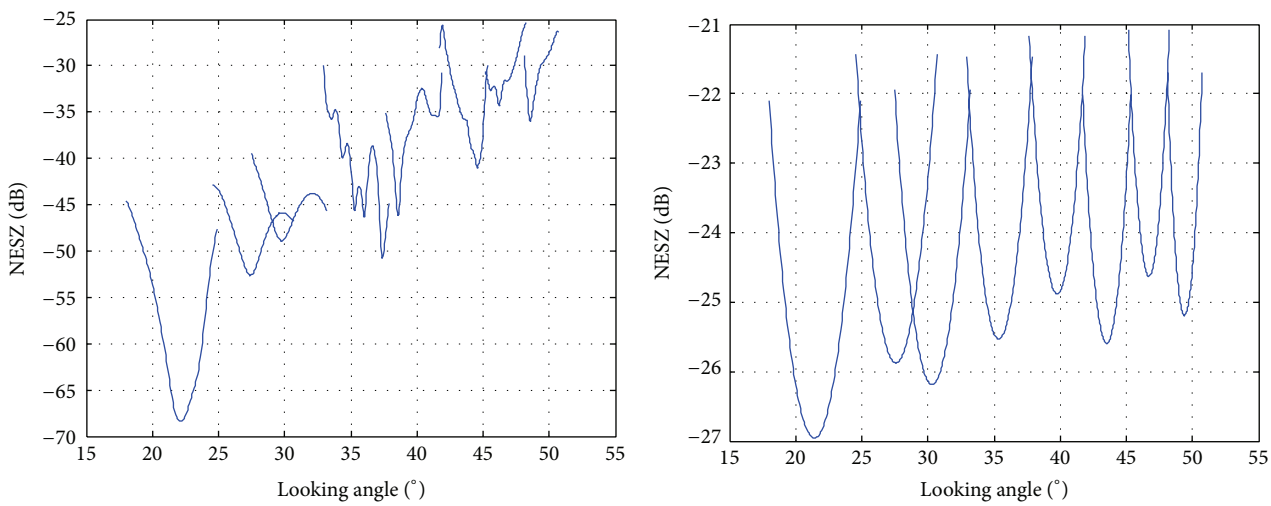

(a) RASR (b) NESZ

Figure 8: System performances of the designed SAR system with the proposed approach.

of each subaperture is first adjusted according the imaging geometry before DBF processing onboard, which results in obviously suppressed grating lobes and the improved RASR level. The only cost of this receive approach is the little NESZ reduction, since the beam pointing direction of each subaperture in elevation is not pointed to the swath center. Furthermore, compared with the improvement of RASR, the NESZ reduction is so little and even could be neglected as shown in Figure 8. Simulation results validate the proposed approach.

Conflict of Interests

The authors declare that there is no conflict of interests regarding the publication of this paper.

Acknowledgments

This work was supported by the National Natural Science Foundation of China under Grant 61201433 and supported by Program for Young Talents of Science and Technology in Universities of Inner Mongolia Autonomous Region (NJYT-14-B09).

References

[1] N. Gebert, *Multi-channel azimuth processing for high-resolution wide-swath SAR imaging [Ph.D. dissertation]*, Universität Karlsruhe, Karlsruhe, Germany, 2009.

[2] A. Currie and M. A. Brown, "Wide-swath SAR," *IEE Proceedings, Part F: Radar and Signal Processing*, vol. 139, no. 2, pp. 122–135, 1992.

[3] W. Xu, Y. Deng, and R. Wang, "Multichannel synthetic aperture radar systems with a planar antenna for future spaceborne microwave remote sensing," *IEEE Aerospace and Electronic Systems Magazine*, vol. 27, no. 12, pp. 26–30, 2012.

[4] G. Krieger, "MIMO-SAR: opportunities and pitfalls," *IEEE Transactions on Geoscience and Remote Sensing*, vol. 52, no. 5, pp. 2628–2645, 2014.

[5] N. Gebert, G. Krieger, and M. A. Moreira, "Digital beamforming on receive: techniques and optimization strategies for high-resolution wide-swath SAR imaging," *IEEE Transactions on Aerospace and Electronic Systems*, vol. 45, no. 2, pp. 564–592, 2009.

[6] G. Krieger, N. Gebert, and A. Moreira, "Multidimensional waveform encoding: a new digital beamforming technique for synthetic aperture radar remote sensing," *IEEE Transactions on Geoscience and Remote Sensing*, vol. 46, no. 1, pp. 31–46, 2008.

[7] M. Suess, B. Grafmueller, and R. Zahn, "A novel high resolution, wide swath SAR system," in *Proceedings of the International Geoscience and Remote Sensing Symposium (IGARRS '01)*, pp. 1013–1015, Sydney, Australia, July 2001.

[8] M. Suess and W. Wiesbeck, "Side-looking synthetic aperture radar system," Euro Patent EP 1 241 487 A1, 2001.

[9] C. Schaefer, C. Heer, and M. Ludwig, "X-band demonstrator for receive-only frontend with digital beamforming," in *Proceedings of the 8th European Conference on Synthetic Aperture Radar (EUSAR '10)*, pp. 1–4, Aachen, Germany, June 2010.

[10] W. Xu and Y. K. Deng, "Multichannel SAR with reflector antenna for high-resolution wide-swath imaging," *IEEE Antennas and Wireless Propagation Letters*, vol. 9, pp. 1123–1126, 2010.

[11] G. Krieger, M. Younis, N. Gebert et al., "Advanced concepts for high-resolution wide-swath SAR imaging," in *Proceedings of the 8th European Conference on Synthetic Aperture Radar (EUSAR '10)*, pp. 1–4, VDE, Aachen, Germany, June 2010.

[12] M. Younis, A. Patyuchenko, S. Huber, and G. Krieger, "Design and optimization aspects for reflector-based synthetic aperture radar," in *Proceedings of the IEEE International Geoscience and Remote Sensing Symposium (IGARSS '11)*, pp. 3967–3970, Vancouver, Canada, July 2011.

[13] J. Kim and W. Wiesbeck, "Investigation of a new multifunctional high performance SAR system concept exploiting MIMO technology," in *Proceedings of the IEEE International Geoscience and Remote Sensing Symposium (IGARSS '08)*, pp. 221–224, Boston, Mass, USA, July 2008.

[14] C. Schaefer, C. Heer, and M. Ludwig, "Advanced C-band instrument based on digital beamforming," in *Proceedings of the 8th European Conference on Synthetic Aperture Radar (EUSAR '10)*, pp. 1–4, Aachen, Germany, June 2010.

[15] D. D'Aria, F. De Zan, D. Giudici, A. M. Guarnieri, and F. Rocca, "Burst-mode SARs for wide-swath surveys," *Canadian Journal of Remote Sensing*, vol. 33, no. 1–4, pp. 27–38, 2007.

[16] F. Feng, S. Li, W. Yu, P. Huang, and W. Xu, "Echo separation in multidimensional waveform encoding SAR remote sensing using an advanced null-steering beamformer," *IEEE Transactions on Geoscience and Remote Sensing*, vol. 50, no. 10, pp. 4157–4172, 2012.

[17] J. C. Curlander and R. N. McDonough, *Synthetic Aperture Radar: Systems and Signal Processing*, Wiley, New York, NY, USA, 1991.